

Gate Driver IC With Fully Integrated Overcurrent Protection for Driving Magnet Reversal Motor With High Pulse Current

Yohei Sukita¹, Haifeng Zhang¹, Dibo Zhang¹, Katsuhiro Hata², Keiji Wada³, Kan Akatsu⁴,
Ichiro Omura⁵, and Makoto Takamiya¹

¹ The University of Tokyo, Tokyo, Japan

² Shibaura Institute of Technology, Tokyo, Japan

³ Tokyo Metropolitan University, Tokyo, Japan

⁴ Yokohama National University, Kanagawa, Japan

⁵ Kyushu Institute of Technology, Fukuoka, Japan

Abstract- Magnet reversal motors (MRMs) are attracting attention as motors based on a new principle that can reduce copper loss. In this paper, overcurrent protection measured results are shown by applying a gate driver IC with a fully integrated overcurrent protection function to IGBTs in a high-current pulse generator circuit to drive an MRM. Since this IC does not require additional external components such as a high-voltage diode for overcurrent detection, it contributes to high reliability and low cost of MRMs that require high-current pulses.

Index Terms— gate driver, motor, overcurrent, protection

I. INTRODUCTION

A magnet reversal motor (MRM) [1] was proposed as a new principle motor that can reduce copper loss. Since high current pulses of, for example, 400 A are required to drive MRM, power devices with high current ratings are needed for the MRM drive circuit, which leads to increased cost. In order to achieve both high reliability and low cost for high current in MRMs, a new overcurrent protection technology called “monitoring gate voltage while periodically repeating discharging and charging of constant gate charge (MGDC)” [2] and full integration of MGDC into a gate driver IC chip [3] were reported. Using the IC, overcurrent protection has been demonstrated for an IGBT module [3] and a SiC module [4], respectively. In this paper, demonstration measurements are performed using the above gate driver IC [3] to drive MRM. Specifically, the overcurrent protection function of this IC is demonstrated for a custom-made IGBT module used in a circuit [5] that drives MRM with high-current pulses.

II. GATE DRIVER IC WITH FULLY INTEGRATED OVERCURRENT PROTECTION

Fig. 1 shows an operation principle of the custom-made gate driver IC [3] with a fully integrated overcurrent protection function by measuring gate-to-emitter voltage (OPV) while IGBTs are ON. Two functions, a periodic constant gate charge (Q_C) discharger and recharger, and an overcurrent protection by gate-to-emitter voltage (V_{GE}),

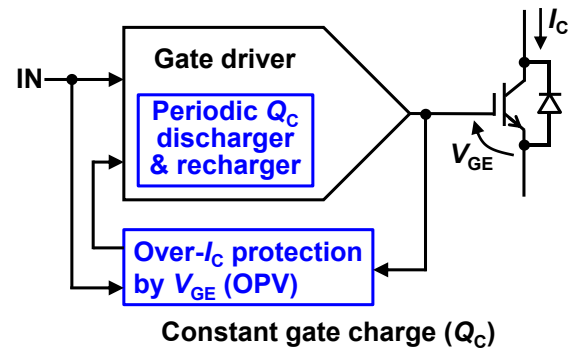


Fig. 1. Operation principle of custom-made gate driver IC [3] with fully integrated overcurrent protection function by measuring V_{GE} (OPV).

are added to the gate driver IC. While the IGBTs are ON, the periodic Q_C discharger and recharger periodically discharges and recharges Q_C . When V_{GE} dropped by each discharge is less than the reference voltage (V_{REF}), it is detected as the overcurrent and the gate driver is forced to turn off to complete the overcurrent protection.

Fig. 2 shows a circuit schematic of the gate driver IC with OPV [3]. All circuits enclosed in a blue square are integrated on a single chip. To achieve the two functions shown in blue in Fig. 1, an OPV circuit is added to our

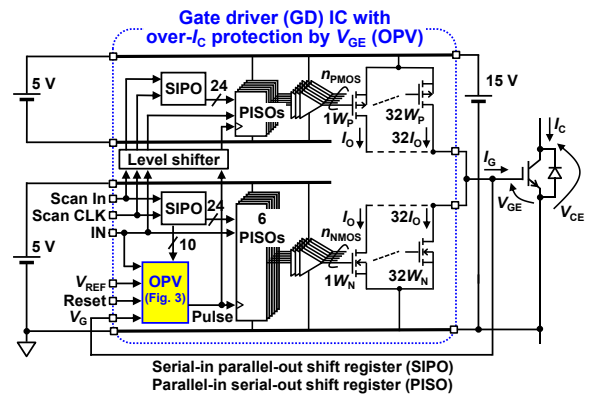


Fig. 2. Circuit schematic of gate driver IC [3] with OPV.

This work was partly supported by JST-Mirai Program, Grant Number JPMJMI20E1, Japan.

previously developed 6-bit current-source type digital gate driver [6, 7] with variable gate current (I_G) in 64 levels, where $I_G = n_{PMOS} \times 48 \text{ mA}$ and n_{PMOS} is an integer from 0 to 63 at turn-on. The 64-level I_G control is achieved by selectively turning on or off six pMOSFETs with binary weighted gate widths ($W_P, 2W_P, 4W_P, 8W_P, 16W_P, 32W_P$) in the output stage depending on the 6-bit control signals for n_{PMOS} [6, 7]. The exact same is true for turn-off by controlling n_{NMOS} .

Fig. 3 shows a circuit schematic of OPV circuit. The OPV circuit include a digitally controlled oscillator (DCO) to determine charging and discharging time and a V_{GE} detector to detect the overcurrent by comparing V_{GE} and V_{REF} .

Figs. 4 and 5 show the timing charts of the conventional and developed overcurrent protection [3], respectively. In the conventional desaturation detection shown in Fig. 4,

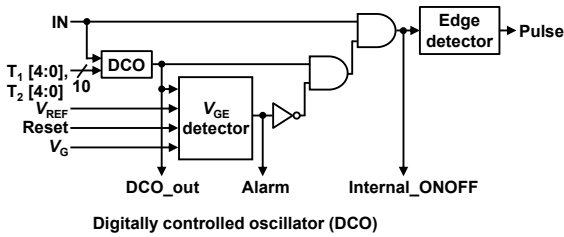


Fig. 3. Circuit schematic of OPV circuit [3].

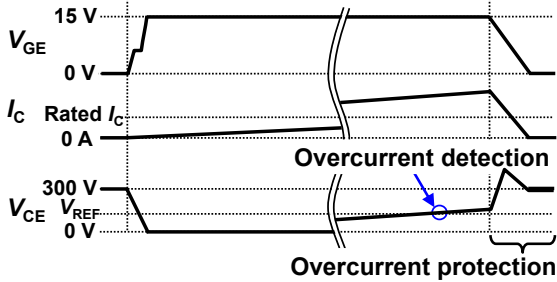


Fig. 4. Timing charts of conventional overcurrent protection.

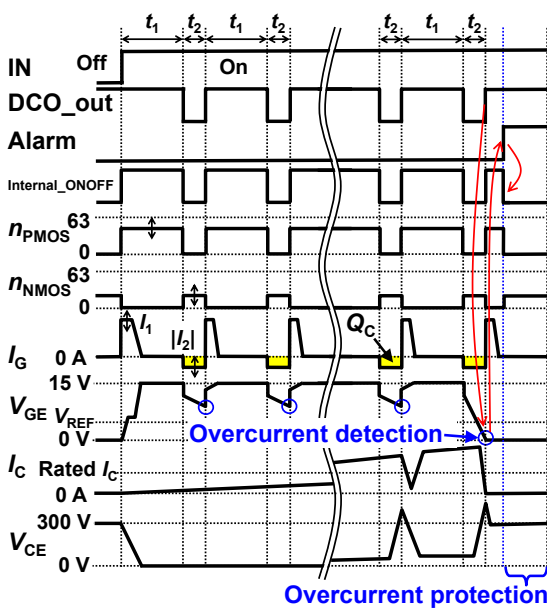


Fig. 5. Timing charts of developed overcurrent protection using MGDC [3].

overcurrent is detected when the collector-to-emitter voltage (V_{CE}) exceeds V_{REF} . In the gate driver IC with OPV [3], the four parameters (t_1, t_2, I_1 , and I_2) in Fig. 5, where t_1 is charging time, t_2 is discharging time, I_1 is charging gate current, and I_2 is discharging gate current, can be digitally controlled to achieve MGDC [2]. All parameters are written in advance to the on-chip memory (two SIPOs in Fig. 2) by scan-in. In the developed overcurrent protection using MGDC shown in Fig. 5, $Q_C (= |I_2| \times t_2)$ is periodically discharged with the $t_1 + t_2$ cycle, and if the resulting drop in V_{GE} is greater than V_{REF} , it is judged normal, and if the resulting drop in V_{GE} is less than V_{REF} , it is judged overcurrent and the IGBTs are immediately turned off to protect from the overcurrent. In the t_1 period after each discharge, V_{GE} is recharged to 15 V.

Fig. 6 shows a photo of a gate driver PCB including the custom-made gate driver IC with OPV [3]. The PCB size is 32 mm by 65 mm.

III. MEASURED RESULTS

Figs. 7 and 8 show a circuit schematic and a photo of the measurement setup for a single-pulse test of a custom-made IGBT module with an inductive load of 34 μH , respectively. The power supply voltage (V_{CC}) is varied. The custom-made IGBT module includes an IGBT (Q_1 : SIGC109T120R3E, 1200 V, 100 A DC, 300 A pulse rating) and a diode (D_1 : IDC51D120T8H, 1200 V, 100 A DC, 200 A pulse rating). The high-side diode (D_2) is GB2X100MPS12-227 (1200 V, 100 A DC, 1000 A pulse rating).

The differences between the IGBTs and gate driver ICs in our prior works [2, 3] and in this paper are described. In [2], compared to the IGBT in this paper, an IGBT with exactly half the current rating and a digital gate driver IC without overcurrent detection and protection function were used. In [2], oscilloscope measurements only demonstrated the operating principle of overcurrent detection using MGDC, and the overcurrent protection function was not demonstrated. In [3], a commercial IGBT module (FF100R12RT4, 1200 V, 100 A DC, 200 A pulse rating) and a gate driver IC identical to the one in this paper were used. Compared to the IGBT in [3], the IGBT in this paper has the same DC current rating and 1.5 times higher pulse current rating.

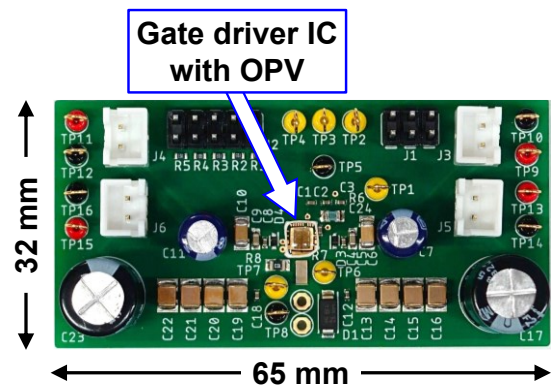


Fig. 6. Photo of gate driver PCB including gate driver IC with OPV [3].

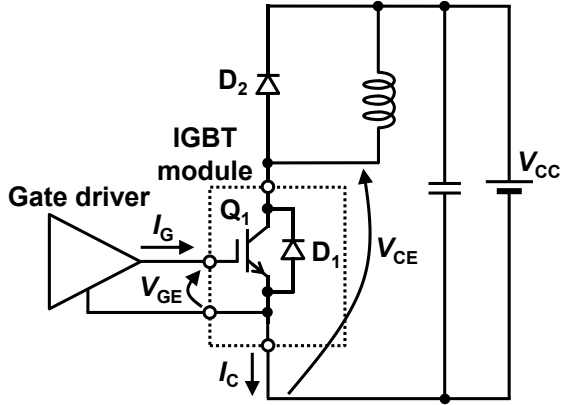


Fig. 7. Circuit schematic of single-pulse test.

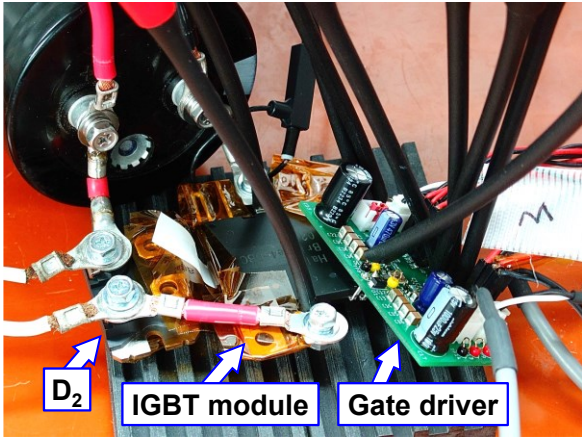


Fig. 8. Photo of measurement setup.

Figs. 9 (a) to (c) show the measured waveforms of the conventional overcurrent at $V_{CC} = 100$ V, 150 V, and 200 V, respectively. In the conventional desaturation detection, the overcurrent is detected by the V_{CE} increases. In Fig. 9, the IGBT is turned off manually.

Figs. 10 (a) to (c) show the measured waveforms of the developed overcurrent protection using the gate driver IC with OPV at $V_{CC} = 100$ V, 150 V, and 200 V, respectively. The MGDC parameters are fixed at $t_1 = 2.5$ μ s, $t_2 = 0.63$ μ s, $I_1 = 1.4$ A, and $|I_2| = 0.77$ A. In Fig. 10, “(1) Q_C discharge in t_2 , (2) comparison of V_{GE} and V_{REF} at the end of t_2 , and (3) recharge to $V_{GE} = 15$ V in t_1 ”, is repeated in $t_1 + t_2$ cycles. When $V_{GE} < V_{REF}$, the overcurrent is detected, Alarm changes from low to high, Internal_ONOFF changes from high to low, and the gate driver is forced to turn off to complete overcurrent protection. The overcurrent protection threshold (I_{TH}) is 336 A to 364 A. The protection delay from overcurrent detection to protection completion is 610 ns to 701 ns.

Table I shows a summary of I_{TH} and the protection delay extracted from Fig. 10. The overcurrent protection is reasonable, because the overcurrent protection with I_{TH} of 336 A to 364 A is performed for the IGBT with a rated pulse current of 300 A. Also, as expected, V_{CC} dependence of I_{TH} and the protection delay is almost negligible, thus overcurrent protection operation is successfully achieved. Specifically, the difference between the maximum and minimum values for I_{TH} is 8% and the difference between

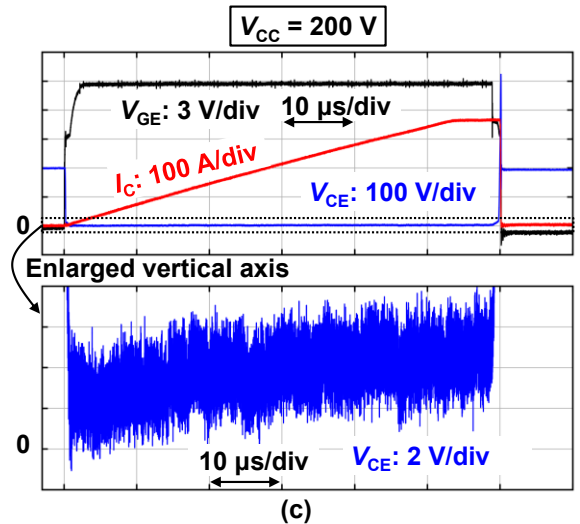
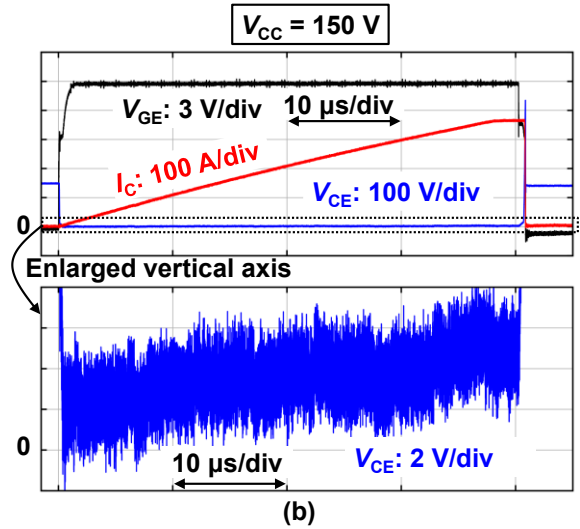
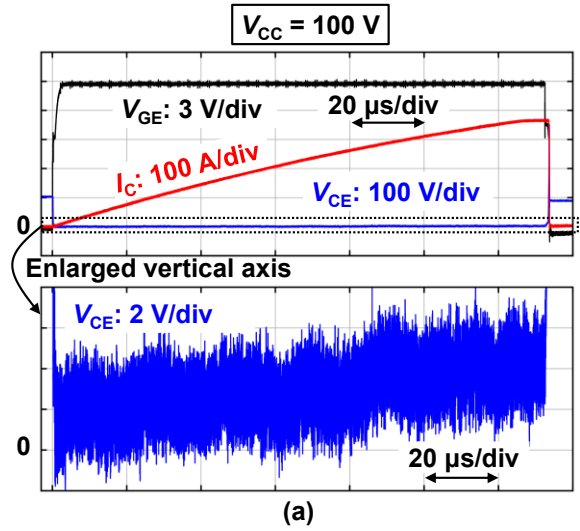


Fig. 9. Measured waveforms of conventional overcurrent. (a) $V_{CC} = 100$ V. (b) $V_{CC} = 150$ V. (c) $V_{CC} = 200$ V.

the maximum and minimum values for the protection delay is 15%.

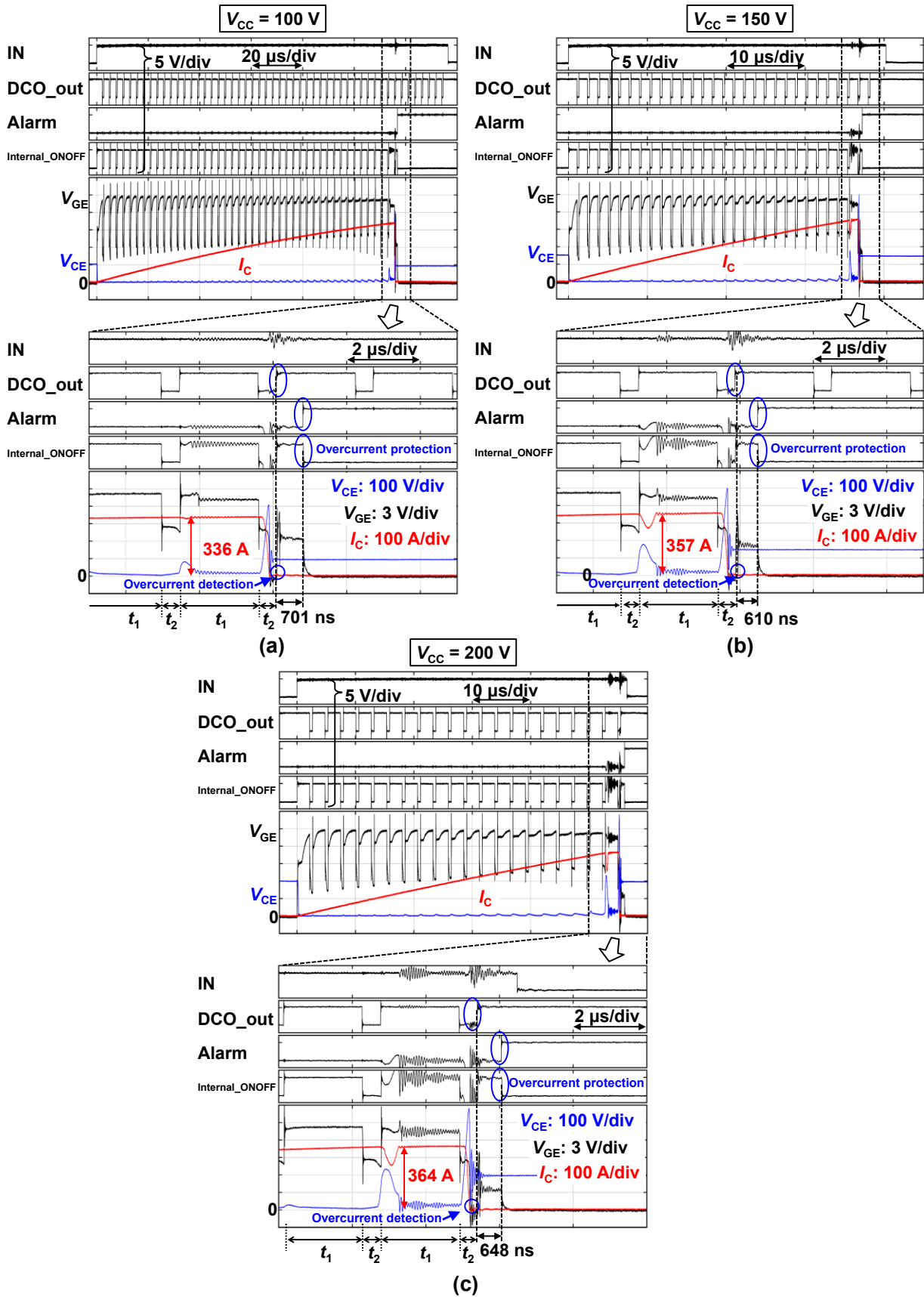


Fig. 10. Measured waveforms of developed overcurrent protection using gate driver IC with OPV. (a) $V_{CC} = 100$ V. (b) $V_{CC} = 150$ V. (c) $V_{CC} = 200$ V.

TABLE I. SUMMARY OF I_{TH} AND PROTECTION DELAY

| V_{CC} | 100 V | 150 V | 200 V |
|--|---------------|---------------|---------------|
| Overcurrent detection threshold (I_{TH}) | 336 A | 357 A | 364 A |
| Protection delay | 701 ns | 610 ns | 648 ns |

IV. CONCLUSIONS

The overcurrent protection function of the gate driver IC [3] was demonstrated for the custom-made IGBT module used in a circuit [5] that drives MRM with high-current pulses. In a single-pulse test of an inductive load at $V_{CC} = 100$ V, 150 V, and 200 V for the IGBT with a pulse rating of 300 A, the developed gate driver IC successfully protected the overcurrent of 336 A to 364 A with the protection delay of 610 ns to 701 ns.

REFERENCES

- [1] Y. Yamada and K. Akatsu, "A new motor with stator magnet using the magnetization reversal technique," in *Proc. 2016 XXII International Conference on Electrical Machines (ICEM)*, 2016, pp. 60–65.
- [2] H. Zhang, H. Yamasaki, K. Hata, I. Omura, and M. Takamiya, "Overcurrent detection method by monitoring gate voltage while periodically repeating discharging and charging of constant gate charge in IGBTs," in *Proc. 2022 IEEE 7th Southern Power Electronics Conference (SPEC)*, 2022, pp. 1–5.
- [3] H. Zhang, H. Yamazaki, K. Hata, I. Omura, and M. Takamiya, "Gate driver IC with fully integrated overcurrent protection function by measuring gate-to-emitter voltage during IGBT conduction," in *Proc. 2023 35th International Symposium on Power Semiconductor Devices and ICs (ISPSD)*, 2023, pp. 76–79.
- [4] H. Zhang, D. Zhang, K. Hata, K. Wada, K. Akatsu, I. Omura, and M. Takamiya, "Fully integrated overcurrent protection method during SiC MOSFET conduction," in *Proc. 2023 IEEE 8th Southern Power Electronics Conference and 17th Brazilian Power Electronics Conference (SPEC/COBEP)*, 2023, pp. 1–8.
- [5] K. Shimo and K. Wada, "Bipolar pulse current magnetizer for driving a magnetization reversal motor," in *IEEJ J. Ind. Appl.*, vol. 11, no. 6, pp. 798–806, 2022.
- [6] K. Horii, R. Morikawa, R. Katada, K. Hata, T. Sakurai, S. Hayashi, K. Wada, I. Omura, and M. Takamiya, "Equalization of DC and surge components of drain current of two parallel-connected SiC MOSFETs using single-input dual-output digital gate driver IC," in *Proc. 2022 IEEE Applied Power Electronics Conference and Exposition (APEC)*, 2022, pp. 1406–1412.
- [7] D. Zhang, K. Horii, K. Hata, and M. Takamiya, "Digital gate driver IC with fully integrated automatic timing control function in stop-and-go gate drive for IGBTs," in *Proc. 2023 IEEE Applied Power Electronics Conference and Exposition (APEC)*, 2023, pp. 1225–1231.